This document describes the dielectric model of InAs employed in our near-field heat transfer calculations [1]. This model is a combination of the work described in Refs. [2], [3], [4], and [5]. Most of the model is adapted from Ref. [2], while the interband absorption calculations are taken from Ref. [3]. To address the overestimation of free carrier absorption, we use the model from Ref. [4]. Finally, we incorporate updated parameters from Ref. [5] and an approximation to the Kramers-Kronig relations, which improves computational speed, as proposed in Ref. [5].

1. Undoped Bandgap

The undoped bangap E_{g}^{0} is calculated using the relation

$$E_{\mathrm{g}}^{0}(T) = E_{\mathrm{g}}^{0}(0) - \frac{\delta T^{2}}{T+\beta},$$

where $E_{\mathrm{g}}^{0}(0)$ is the undoped zero temperature bandgap. We use the following values [6]:

$E_{\mathrm{g}}^{0}(0) = 0.417$ eV,

$\delta = 2.76 \times 10^{-4}$ eV/K,

$\beta = 93$ K.

2. Electron and Hole Effective Masses

We compute the electron and hole effective masses using the following expressions [7]

$$m_{\mathrm{e}}^{*} = 0.024 \cdot m_{0},$$

$$m_{\mathrm{h}}^{*} = \left(m_{\mathrm{hh}}^{3/2} + m_{\mathrm{lh}}^{3/2}\right)^{2/3},$$

where m_{0} is the mass of an electron and m_{hh} and m_{lh} are the heavy-hole and light-hole effective masses, respectively,

$$m_{\mathrm{hh}} = 0.57 \cdot m_{0},$$

$$m_{\mathrm{lh}} = 0.026 \cdot m_{0}.$$

The value of m_{hh} is taken from Ref. [8] and the value of m_{lh} is taken from Ref. [9]. From this point on we will only refer to m^{*}. In the case of n-doped $m^{*} = m_{\mathrm{e}}^{*}$ and for p-doped $m^{*} = m_{\mathrm{h}}^{*}$.

3. Carrier Mobility

The carrier mobility μ is computed using the following equation:

$$\mu(N,T) = \mu_{\mathrm{min}} + \frac{\mu_{\mathrm{max}}\left(\frac{300}{T}\right)^{\theta_{1}} - \mu_{\mathrm{min}}}{1 + \left(\frac{N_{\mathrm{d}}}{N_{\mathrm{ref}}\left(\frac{T}{300}\right)^{\theta_{2}}}\right)^{\phi}},$$

where N_{d} is the doping level and T is the temperature in Kelvin. Note that, here, we are not using the same parameters as in Ref. [2], we are using the updated parameters from Ref. [5]. In the case of n-doped InAs we use the following parameters:

$$\mu_{\max} = 30\,636.0\ \mathrm{cm^2V^{-1}s^{-1}},$$

$$\mu_{\min} = 0.3\ \mathrm{cm^2V^{-1}s^{-1}},$$

$$N_{\mathrm{ref}} = 3.56\ \times 10^{17}\ \mathrm{cm^{-3}},$$

$$\phi = 0.68,$$

$$\theta_1 = 1.57,$$

$$\theta_2 = 3.0.$$

In the case of p-doped InAs we use the following parameters:

$$\mu_{\max} = 530.0\ \mathrm{cm^2V^{-1}s^{-1}},$$

$$\mu_{\min} = 20\ \mathrm{cm^2V^{-1}s^{-1}},$$

$$N_{\mathrm{ref}} = 1.1\ \times 10^{17}\ \mathrm{cm^{-3}},$$

$$\phi = 0.46,$$

$$\theta_1 = 2.3,$$

$$\theta_2 = 3.0.$$

4. Carrier Concentration

In this section we show how to compute the carrier concentration based on the doping level while considering the contribution of thermally excited carriers using the model described in Chapter 2 of Ref. [10]. There is a flag named *N_calc_choice* in the *main.py* file that determines whether the carrier concentration should be set equal to the doping concentration or to also include thermally-generated carriers.

We first compute the standard effective density of states for parabolic bands in the conduction and valence band, respectively,

$$N_{\mathrm{C}} = 2\left(\frac{2\pi m_{\mathrm{e}}^{*} k_{\mathrm{B}} T}{h^2}\right)^{\frac{3}{2}},$$

$$N_{\mathrm{V}} = 2\left(\frac{2\pi m_{\mathrm{h}}^{*} k_{\mathrm{B}} T}{h^2}\right)^{3/2},$$

where k_{B} is the Boltzmann constant and h is the planck constant. One can then compute the density of thermally excited free electrons and holes

$$N_{\mathrm{th}}^2 = N_{\mathrm{C}} N_{\mathrm{V}} \exp\left(-\frac{E_{\mathrm{g}}^{0}(T)}{k_{\mathrm{B}} T}\right).$$

Finally, the majority carrier concentration is given by

$$N = \frac{1}{2}\left(N_{\mathrm{d}} + \sqrt{N_{\mathrm{d}}^2 + 4 \cdot N_{\mathrm{th}}^2}\right).$$

5. Lattice Response

We compute the lattice contribution to the permittivity using a Lorentz model

$$\varepsilon_{\mathrm{Lattice}}(\omega) = \varepsilon_{\infty}\left(1 + \frac{\omega_{\mathrm{LO}}^2 - \omega_{\mathrm{TO}}^2}{\omega_{\mathrm{TO}}^2 - \omega^2 - i\omega\gamma}\right),$$

where ω is the frequency, γ is the phononic damping coefficient, ω_{LO} is the longitudinal optical phonon frequency, and ω_{TO} is the transverse optical phonon frequency.

We are using the following parameters:

$$\gamma = 9.23 \times 10^{11}\ \mathrm{rad/s},$$

$$\omega_{\mathrm{LO}} = 4.55 \times 10^{13}\ \mathrm{rad/s},$$

$$\omega_{\mathrm{TO}} = 4.14 \times 10^{13}\ \mathrm{rad/s},$$

$$\varepsilon_{\infty} = 11.6.$$

Here, γ is taken from Ref. [11], while ω_{LO} and ω_{TO} are taken from Ref. [12], and $\varepsilon_{\infty} = 11.6$ is taken from Ref. [13].

6. Free Carrier Response

The models of Refs. [5] and [2] used a Drude model for the free-carrier response. Our main change from those models is the replacement of the Drude model with an ionized-impurity-scattering model at high doping levels and high frequency.

6.1. Drude Model

In the case of low doping, p-doped or at low frequency, we calculate the free carrier contribution using the standard Drude model

$$\varepsilon_{\mathrm{Drude}}(\omega, N_{\mathrm{d}}, T) = \varepsilon_{\infty}\left(1 - \frac{\omega_{\mathrm{p}}^2(N_{\mathrm{d}})}{\omega\left(\omega + i\Gamma(N_{\mathrm{d}}, T)\right)}\right),$$

where Γ is the damping coefficient due to free carriers

$$\Gamma(N_{\mathrm{d}}, T) = \frac{e}{m^* \cdot \mu(N_{\mathrm{d}}, T)},$$

and ω_{p} is the plasma resonance

$$\omega_{\mathrm{p}}^2(N_{\mathrm{d}}) = \frac{e^2}{\varepsilon_{\infty}\varepsilon_0}\frac{N}{m^*},$$

where e is the elementary charge, N is the carrier concentration, and ε_0 is the vacuum permittivity. Section 4 shows how to compute the carrier concentration.

6.2. Overestimation of Free Carrier Absorption

The Drude model overestimates absorption from free carriers in n-type InAs at frequencies above the band gap [1]. In the case of highly n-doped InAs at frequencies above ω_p, we use the ionized-impurity scattering model from Ref. [4] to address this overestimation. This model only allows to compute the imaginary part of the permittivity; therefore, we compute the real part of the permittivity ε'_FC using the Drude model. This model is only valid when $k_\mathrm{B}T \ll E_\mathrm{F}$ and $\omega \gg \omega_\mathrm{p}$. The imaginary component is given by

$$\varepsilon''_2(\omega) = A\zeta^{-4}\int_{(1-\zeta)\theta(1-\zeta)}^{1}\left[\frac{1}{2}\ln\frac{\left(\sqrt{X+\zeta}+\sqrt{X}\right)^2+X_\mathrm{TF}}{\left(\sqrt{X+\zeta}-\sqrt{X}\right)^2+X_\mathrm{TF}} - \frac{2X_\mathrm{TF}\sqrt{X(X+\zeta)}}{\left[\left(\sqrt{X+\zeta}+\sqrt{X}\right)^2+X_\mathrm{TF}\right]\left[\left(\sqrt{X+\zeta}-\sqrt{X}\right)^2+X_\mathrm{TF}\right]}\right]dX,$$

where

$$\zeta = \frac{\hbar\omega}{E_\mathrm{F}},$$

$$X_\mathrm{TF} = \left(\frac{q_\mathrm{TF}}{k_\mathrm{F}}\right)^2,$$

$$q_\mathrm{TF} = \sqrt{\frac{3Ne^2}{2\varepsilon_0\varepsilon_\infty E_\mathrm{F}}},$$

$$A = \frac{1}{12\pi^3}\frac{e^2\gamma k_\mathrm{F}^4}{\varepsilon_0 E_\mathrm{F}^3}.$$

Note that we include a $\frac{1}{4\pi\varepsilon_0}$ term in the formulas from Ref. [4] to use SI units. Here, $\hbar$ is the reduced Planck constant and θ is a step function such that

$$\theta(x) = \begin{cases} 0, & x < 0 \\ 1, & x \geq 0 \end{cases}.$$

We are using the Fermi level E_F measured from the conduction band minimum, such that $E_\mathrm{F} = F - E_\mathrm{g}$. We use the model derived from Ref. [2] to find the fermi level F (see Section 7). The Fermi wavevector k_F is

$$k_\mathrm{F} = \frac{\sqrt{2m_\mathrm{e}^* E_\mathrm{F}}}{\hbar}.$$

We can use the following to compute γ

$$\gamma = R\left[\frac{Ze^2}{\varepsilon_0\varepsilon_\infty k_\mathrm{F}^2}\right]^2.$$

Here, R is the number of impurities with charge Ze such that

$$R = ZN_\mathrm{d},$$

where Z is the charge number of impurities. In this case, we use $Z = 1$.

Using this form for $\varepsilon''_\mathrm{FC}$, we could employ the Kramers-Kronig relations to compute the real part of the permittivity ε'_FC, as described in Section 10. However, we have confirmed that simply using ε'_FC from the original Drude model introduces less than 1% error in ε'_FC. The accompanying code has a flag named *model_choice* in the *main.py* file that determines whether to use the Drude ε'_FC or the Kramers-Kronig ε'_FC from $\varepsilon''_\mathrm{FC}$.

6.3. Combined free carrier model

Here is a description of the algorithm to obtain the free-carrier contributions to the dielectric. At low energy $E_\mathrm{F} < k_\mathrm{B}T$ or low frequency $\omega < \omega_\mathrm{p}$ (i.e., region for which the model from Ref. [4] is not valid), we employ the Drude model. Where $E_\mathrm{F} > k_\mathrm{B}T$ and $\omega > \omega_\mathrm{p}$ (i.e., at high doping and high frequency), we employ the model from Ref. [4]. The model from Ref. [4] is also only valid for n-doped semiconductors, we therefore employ the Drude model in the case of p-doped InAs. Here is a description of the algorithm for each ω:

`If` $E_\mathrm{F} > k_\mathrm{B}T$ `and n-type and` $\omega > \omega_\mathrm{p}$`:`

$\varepsilon''_\mathrm{FC}(\omega) = \varepsilon''_2(\omega)$

`If model_choice == “Kramers-Kronig”:`

$$\varepsilon'_\mathrm{FC}(\omega) = \varepsilon'_\mathrm{Drude}(\omega) + H\left((\varepsilon''_2 - \varepsilon''_\mathrm{Drude})\theta(\omega - \omega_p)\right)(\omega).$$

`Else:`

$$\varepsilon'_\mathrm{FC}(\omega) = \varepsilon'_\mathrm{Drude}(\omega))$$

$\varepsilon_\mathrm{FC}(\omega) = \varepsilon'_\mathrm{FC}(\omega) + i \cdot \varepsilon''_\mathrm{FC}(\omega)$

`Else:`

$\varepsilon_\mathrm{FC}(\omega) = \varepsilon_\mathrm{Drude}(\omega)$

As previously mentioned, the flag *model_choice* allows the user to either use the Kramers-Kronig relations to find ε'_FC from $\varepsilon''_\mathrm{FC}$, or approximate $\varepsilon'_\mathrm{FC} = \varepsilon'_\mathrm{Drude}$ to improve computational speed. This approximation was shown to introduce less than 1% error in ε'_FC. The implementation of the Kramers-Kronig relations is discussed in Section 10.

7. Interband Response

The interband response is the same as in Ref. [3]. In this section we use $E_\mathrm{g} = E_\mathrm{g}^0(T)$. First, we calculate k_ω

$$k_\omega^2 = \frac{\left[\frac{4}{3}P^2 + \frac{\hbar^2 E_\mathrm{g}}{m_0}\left(1+\frac{m_0}{m_\mathrm{hh}}\right)\left(\frac{2\hbar\omega}{E_\mathrm{g}}-1\right)\right]}{\frac{\hbar^4}{m_0^2}\left(1+\frac{m_0}{m_\mathrm{hh}}\right)^2} \times \left[1 - \sqrt{1 - \frac{\frac{4\hbar^4}{m_0^2}\left(1+\frac{m_0}{m_\mathrm{hh}}\right)^2 \hbar\omega\left(\hbar\omega - E_\mathrm{g}\right)}{\left[\frac{4}{3}P^2 + \frac{\hbar^2 E_\mathrm{g}}{m_0}\left(1+\frac{m_0}{m_\mathrm{hh}}\right)\left(\frac{2\hbar\omega}{E_\mathrm{g}}-1\right)\right]^2}}\right],$$

where $P = 9.05 \times 10^{-8}\ \mathrm{eV \cdot cm}$, which is taken from Ref. [6].

Now we can calculate the light hole and heavy hole absorption

$$\alpha_\mathrm{lh} = \frac{\left[1 + 2\left(\frac{E_\mathrm{g}}{\hbar\omega}\right)^2\right]}{137\sqrt{6}\sqrt{\epsilon_\infty}} \frac{\sqrt{(\hbar\omega)^2 - E_\mathrm{g}^2}}{4P},$$

$$\alpha_\mathrm{hh} = \frac{1}{137\sqrt{\varepsilon_\infty}} \frac{\frac{E_\mathrm{g}}{\hbar\omega}\frac{k_\omega}{2}\left[\sqrt{1 + \frac{8P^2k_\omega^2}{3E_\mathrm{g}^2}} + 1\right]}{1 + \frac{3}{4}\frac{\hbar^2}{m_0}\frac{E_\mathrm{g}}{P^2}\left(1+\frac{m_0}{m_\mathrm{hh}}\right)\sqrt{1 + \frac{8P^2k_\omega^2}{3E_\mathrm{g}^2}}}.$$

Note that the α_lh expression is based on $k \cdot p$ theory and is therefore only valid near the absorption edge. In this case, the light-hole absorption obeys $\alpha_\mathrm{lh}(\omega) \sim \omega$ as $\omega \to \infty$, leading to a non-convergent Kramers-Kronig relation. This limit is not physical; therefore, we apply a smooth cutoff to send $\alpha_\mathrm{lh}(\omega)$ to zero at large ω, beginning at 0.75 eV, which is the energy at which the split-off hole absorption would begin to contribute to $\alpha(\omega)$. We apply a cutoff over a range of 1 eV. We consider

$$h(\omega) = 1 - g\left(\frac{\omega - \omega_0}{\delta}\right),$$

with

$$g(x) = \frac{f(x)}{f(x) + f(1-x)},$$

$$f(x) = \begin{cases} e^{-\frac{1}{x}} & \text{for } x > 0 \\ 0 & \text{for } x \le 0 \end{cases}.$$

We therefore use $\omega_0 = 0.75$ eV and $\delta = 1$ eV. The behavior of $g(x)$ is illustrated in the following plot.

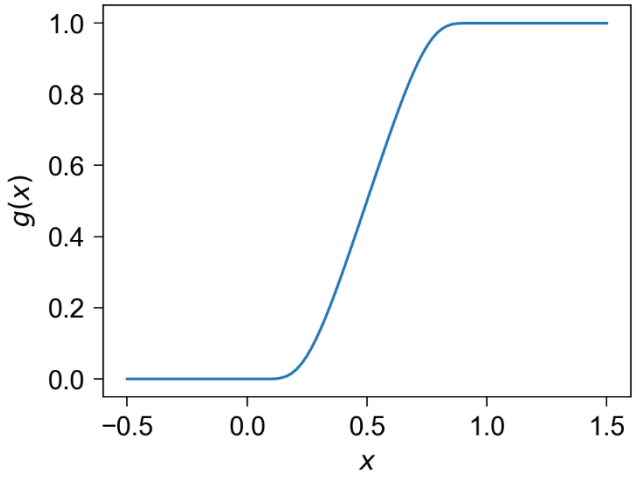

In the case of n-doped InAs, including the effects of non-parabolic corrections to the band and degenerate statistics, the Fermi level F is found by solving the following equation,

$$\frac{N}{N_\mathrm{c}} = \frac{2}{\sqrt{\pi}} \int_0^\infty \frac{x^{\frac{1}{2}} \left(1 + \frac{x}{\phi}\right)^{\frac{1}{2}} \left(1 + \frac{2x}{\phi}\right) dx}{1 + \exp(x - t)},$$

where

$$N_\mathrm{c} = 2\left(\frac{3E_\mathrm{g} k_\mathrm{B} T}{8\pi P^2}\right)^{3/2},$$

$$\phi = \frac{E_\mathrm{g}}{k_\mathrm{B} T},$$

$$t = \frac{F - E_\mathrm{g}}{k_\mathrm{B} T},$$

We solve this equation by minimizing the difference between the actual result and the computed value of the integral. This model is taken from Ref. [3] but was originally developed in Ref. [14]. Note that a non-parabolic band approximation is already included in the N/N_c equation, derived from the Kane relation. For more information, see Ref. [14]. Section 4 shows how to compute the carrier concentration.

The Burstein-Moss shift changes the absorption coefficient when the carrier concentration is large enough to fill the bottom of the bands. We compute the Burstein-Moss shift for the light hole and heavy hole bands using the model from Ref. [3],

$$BM_\mathrm{lh} = \frac{1 - \exp\left(-\frac{\hbar\omega}{k_\mathrm{B} T}\right)}{\left[1 + \exp\left(-\frac{\hbar\omega + E_\mathrm{g} - 2F}{2k_\mathrm{B} T}\right)\right]\left[1 + \exp\left(-\frac{\hbar\omega - E_\mathrm{g} + 2F}{2k_\mathrm{B} T}\right)\right]},$$

$$BM_{\mathrm{hh}} = \frac{1 - \exp\left(-\frac{\hbar\omega}{k_{\mathrm{B}}T}\right)}{\left[1 + \exp\left(-\frac{F + \left(\frac{\hbar^2 k_\omega^2}{2m_{\mathrm{hh}}}\right)}{k_{\mathrm{B}}T}\right)\right]\left[1 + \exp\left(-\frac{\hbar\omega - F - \left(\frac{\hbar^2 k_\omega^2}{2m_{\mathrm{hh}}}\right)}{k_{\mathrm{B}}T}\right)\right]}.$$

The Burstein-Moss shift is primarily of interest in n-doped semiconductors [3] and, therefore, will not be considered in the case of p-doped InAs. We can then compute the interband permittivity using the following algorithm:

If $\omega < E_g$:

$\alpha_{\mathrm{IB}}(\omega) = 0.0$

Else:

If n-type:

$\alpha_{\mathrm{IB}}(\omega) = \alpha_{\mathrm{lh}}(\omega) * BM_{\mathrm{lh}}(\omega) * h(\omega) + \alpha_{\mathrm{hh}}(\omega) * BM_{\mathrm{hh}}(\omega)$

Else: # we do not need the Burstein-Moss shift for p-type

$\alpha_{\mathrm{IB}}(\omega) = \alpha_{\mathrm{lh}}(\omega) * h(\omega) + \alpha_{\mathrm{hh}}(\omega)$

$n''_{\mathrm{IB}}(\omega) = \frac{\alpha_{\mathrm{IB}}(\omega)c}{2\omega}$

If model_choice == “Kramers-Kronig”:

$n'_{\mathrm{IB}}(\omega) = \sqrt{\varepsilon_\infty} + H(n''_{\mathrm{IB}})(\omega)$

Else:

$n'_{\mathrm{IB}}(\omega) = \sqrt{\varepsilon_\infty}$

$\varepsilon_{\mathrm{IB}}(\omega) = (n'_{\mathrm{IB}}(\omega)^2 - n''_{\mathrm{IB}}(\omega)^2) + i2n'_{\mathrm{IB}}(\omega)n''_{\mathrm{IB}}(\omega)$

Note: Here, the flag *model_choice* allows the user to either use the Kramers-Kronig relations to find n'_{IB} from n''_{IB}, as was done in Ref. [2], or approximate $n'_{\mathrm{IB}} = \sqrt{\varepsilon_\infty}$, following the approach of Ref. [5], to improve computational speed. This approximation was shown to have a negligible impact in Ref. [5]. The implementation of the Kramers-Kronig relations is discussed in Section 10.

8. Total Permittivity

To compute the total permittivity, one must first determine the susceptibility from each contribution

$$\chi_{\mathrm{FC}} = \varepsilon_{\mathrm{FC}} - \varepsilon_\infty,$$

$$\chi_{\mathrm{Lattice}} = \varepsilon_{\mathrm{Lattice}} - \varepsilon_\infty,$$

$$\chi_{\mathrm{IB}} = \varepsilon_{\mathrm{IB}} - \varepsilon_\infty,$$

where χ_{FC} is the susceptibility due to free carrier absorption, χ_{Lattice} is the susceptibility due to lattice vibrations, and χ_{IB} is the susceptibility due to interband transitions. The total permittivity is then given by

$$\varepsilon_{tot} = \varepsilon_{\infty} + \chi_{\mathrm{FC}} + \chi_{\mathrm{Lattice}} + \chi_{\mathrm{IB}}.$$

9. Forcade 2022 [5] vs Milovich 2020 [2]

Here is a table showing the differences in the model parameters employed in Ref. [5] and the one of Ref. [2]. The model described above relies on the parameters from Ref. [5].

Variable	**Model Section**	**Ref.** [5]	**Ref.** [2]
$\mu_{\mathrm{max,e}}\ [\mathrm{cm^2V^{-1}s^{-1}}]$	Carrier Mobility	30,636	34,000
$\mu_{\mathrm{min,e}}\ [\mathrm{cm^2V^{-1}s^{-1}}]$	Carrier Mobility	0.3	1000
$N_{\mathrm{ref,e}}\ [\mathrm{cm^{-3}}]$	Carrier Mobility	3.56×10^{17}	1.1×10^{18}
ϕ_{e}	Carrier Mobility	0.68	0.32
$\gamma\ [\mathrm{rad/s}]$	$\varepsilon_{\mathrm{FCL}}$	9.23×10^{11}	2.89×10^{11}
$\omega_{\mathrm{LO}}\ [\mathrm{rad/s}]$	$\varepsilon_{\mathrm{FCL}}$	4.55×10^{13}	4.58×10^{13}
$\omega_{\mathrm{TO}}\ [\mathrm{rad/s}]$	$\varepsilon_{\mathrm{FCL}}$	4.14×10^{13}	4.12×10^{13}
m_{e}^{*}	$\varepsilon_{\mathrm{FCL}}$	$0.024m_0$	$0.026m_0$
m_{hh}^{*}	$\varepsilon_{\mathrm{FCL}}$ and $\varepsilon_{\mathrm{IB}}$	$0.57m_0$	$0.41m_0$
ε_{∞}	-	11.6	11.7
$P\ [\mathrm{eV \cdot cm^{-1}}]$	$\varepsilon_{\mathrm{IB}}$	9.05×10^{-8}	8.58×10^{-8}
m'_{IB}	$\varepsilon_{\mathrm{IB}}$	$\sqrt{\varepsilon_{\infty}}$	Kramers-Kronig relations

10. Kramers-Kronig Relations

While Ref. [1] did not use the Kramers-Kronig relations to compute the permittivity in the heat transfer calculations, they were implemented to verify our approximations for the free-carrier and interband models. Additionally, they are optional in the permittivity algorithm. Here is how they are implemented.

10.1. Standard Kramers-Kronig Relations

The basic Kramers-Kronig relation takes the following form

$$\varepsilon'(\omega) = \varepsilon_{\infty} + \frac{2}{\pi}\mathcal{P}\int_0^{\infty} \frac{\Omega\varepsilon''(\Omega)}{\Omega^2 - \omega^2}\mathrm{d}\Omega,$$

where $\mathcal{P}$ indicates that the integral is a principal value integral. Unfortunately, this integral must be performed for all frequencies, which can be computationally expensive if performed inefficiently. We therefore opt to employ the Hilbert transform to improve the computational speed. The continuous Hilbert transform takes the following form

$$H(u)(t) = \frac{1}{\pi}\mathcal{P}\int_{-\infty}^{+\infty} \frac{u(\tau)}{\tau - t}\mathrm{d}\tau.$$

However, with τ sampled at discrete set of points, we employ the discrete Hilbert transform as implemented in the python function *scipy.fftpack.hilbert()*. The Kramers-Kronig relations are derived from

the Hilbert transform pair so we can easily express the Kramers-Kronig relations as a function of the Hilbert transform

$$\varepsilon'(\omega) = \varepsilon_\infty + H(\varepsilon'')(\omega).$$

The discrete Hilbert transform can be evaluated efficiently using the fast Fourier transform. It is evaluated once and gives the result at all frequencies on the user's input frequency mesh.

10.2. Kramers-Kronig for Free Carrier Model

The model described in Section 6.2 employs the imaginary part of the Drude model for $\omega < \omega_p$. We can write the resulting imaginary contribution to the permittivity as

$$\varepsilon''_{\mathrm{FC}} = \varepsilon''_{\mathrm{Drude}}\Big(1 - \theta\big(\omega - \omega_p\big)\Big) + \varepsilon''_2\theta\big(\omega - \omega_p\big),$$

From this form, we would normally evaluate $\varepsilon'_{\mathrm{FC}}$ from $\varepsilon''_{\mathrm{FC}}$ as

$$\varepsilon'_{\mathrm{FC}} = \varepsilon_\infty + H(\varepsilon''_{\mathrm{FC}})(\omega).$$

However, the Drude model has a pole at $\omega = 0$, which needs to be handled separately in the Kramers-Kronig relations [15]. Since the Drude model is already causal (i.e., its real and imaginary parts are already Kramers-Kronig dual), the Kramers-Kronig conjugate of $\varepsilon''_{\mathrm{Drude}}$ is just $\varepsilon'_{\mathrm{Drude}}$,

$$\varepsilon'_{\mathrm{Drude}} = \varepsilon_\infty + H(\varepsilon''_{\mathrm{Drude}})(\omega).$$

Therefore, we can write

$$\varepsilon'_{\mathrm{FC}} = \varepsilon'_{\mathrm{Drude}} + H\Big((\varepsilon''_2 - \varepsilon''_{\mathrm{Drude}})\theta\big(\omega - \omega_p\big)\Big)(\omega).$$

Note that this Hilbert transform no longer involves evaluating $\varepsilon''_{\mathrm{Drude}}$ at $\omega = 0$, which removes the problem of the pole. Here, the ε_∞ component is included in $\varepsilon'_{\mathrm{Drude}}$.

Also note that we must antisymmetrize ε'' in order to compute the Hilbert transform. We therefore perform the following operation before performing the Hilbert transform.

```
eps_FC_full = np.concatenate((-eps_FC[::-1], eps_FC))
```

If we were using the Kramers-Kronig relations to calculate ε'' from ε', we would instead need to symmetrize ε'.

10.3. Kramers-Kronig for Interband Model

In the case of the interband model, we can perform the Kramers-Kronig relations to find the real part of the refractive index n'_{IB} from the imaginary part n''_{IB}. In the case of the refractive index the Kramers-Kronig relations take the following form

$$n'_{\mathrm{IB}} = \sqrt{\varepsilon_\infty} + \frac{1}{\pi}\mathrm{P}\int_{-\infty}^{+\infty}\frac{n''_{\mathrm{IB}}(\Omega)}{\Omega - \omega}\,\mathrm{d}\Omega.$$

We can therefore perform the following

$$n'_{\mathrm{IB}}(\omega) = \sqrt{\varepsilon_\infty} + H(n''_{\mathrm{IB}})(\omega).$$

Note that, here, we must antisymmetrize n'' like we did for the free carrier contribution

```
n_IB_full = np.concatenate((-n_IB[::-1], n_IB))
```

10.4. Computing the Total Permittivity

To summarize, we obtain the real part of the permittivity or refractive index from the free carrier and interband models as follows

$$\varepsilon'_{\mathrm{FC}} = \varepsilon'_{\mathrm{Drude}} + H\left((\varepsilon''_2 - \varepsilon''_{\mathrm{Drude}})\theta(\omega - \omega_p)\right)(\omega),$$

$$n'_{\mathrm{IB}}(\omega) = \sqrt{\varepsilon_\infty} + H(n''_{\mathrm{IB}})(\omega).$$

We can then combine the real and imaginary part of each model as follows

$$\varepsilon_{\mathrm{FC}}(\omega) = \varepsilon'_{\mathrm{FC}}(\omega) + i \cdot \varepsilon''_{\mathrm{FC}}(\omega),$$

$$n_{\mathrm{IB}}(\omega) = n'_{\mathrm{IB}}(\omega) + i \cdot n''_{\mathrm{IB}}(\omega).$$

Then, from the interband refractive index we can find the interband permittivity

$$\varepsilon_{\mathrm{IB}} = n^2_{\mathrm{IB}}.$$

We can then compute the susceptibility from each contribution

$$\chi_{\mathrm{FC}} = \varepsilon_{\mathrm{FC}} - \varepsilon_\infty,$$

$$\chi_{\mathrm{Lattice}} = \varepsilon_{\mathrm{Lattice}} - \varepsilon_\infty,$$

$$\chi_{\mathrm{IB}} = \varepsilon_{\mathrm{IB}} - \varepsilon_\infty,$$

Finally, we can combine these components to obtain the total permittivity

$$\varepsilon_{tot} = \varepsilon_\infty + \chi_{\mathrm{FC}} + \chi_{\mathrm{Lattice}} + \chi_{\mathrm{IB}}.$$

References

[1] M. Giroux, S. Molesky, R. St-Gelais and J. J. Krich, "Radiator Tailoring for Enhanced Performance in InAs-Based Near-Field Thermophotovoltaics," *arXiv,* 2025.

[2] D. Milovich, J. Villa, E. Antolin, A. Datas, A. Marti, R. Vaillon and M. Francoeur, "Design of an indium arsenide cell for near-field thermophotovoltaic devices," *Journal of Photonics for Energy,* pp. 025503-025503, 2020.

[3] W. W. Anderson, "Absorption constant of Pb1−xSnxTe and Hg1−xCdxTe alloys," *Infrared Physics,* vol. 20, pp. 363-372, 1980.

[4] R. von Baltz and W. Escher, "Quantum Theory of Free Carrier Absorption," *physica status solidi (b),* vol. 51, pp. 499-507, 1972.

[5] G. P. Forcade, C. E. Valdivia, S. Molesky, S. Lu, A. W. Rodriguez, J. J. Krich, R. St-Gelais and K. Hinzer, "Efficiency-optimized near-field thermophotovoltaics using InAs and InAsSbP," *Applied Physics Letters,* vol. 121, p. 193903, 2022.

[6] I. Vurgaftman, J. R. Meyer and L. R. Ram-Mohan, "Band parameters for III–V compound semiconductors and their alloys," *Journal of Applied Physics,* vol. 89, p. 5815–5875, 2001.

[7] S. Adachi, Handbook on physical properties of semiconductors, Springer Science & Business Media, 2004.

[8] J. Piprek, Semiconductor optoelectronic devices: Introduction to physics and simulations, Elsevier, 2013.

[9] M. E. Levinshteın, S. L. Rumyantsev and M. Shur, Handbook series on semiconductor parameters: volume 1: Si, Ge, C (Diamond), GaAs, GaP, GaSb, InAs, InP, InSb, World Scientific, 1996.

[10] S. M. Sze, Physics of semiconductor devices, John Wiley & Sons, 1969.

[11] S. Adachi, Optical Properties of Crystalline and Amorphous Semiconductors: Materials and Fundamental Principles, New York, NY: Springer, 1999.

[12] S. Adachi, Properties of semiconductor alloys: group-IV, III-V and II-VI semiconductors, John Wiley & Sons, 2009.

[13] S. Adachi, "III-V Ternary and Quaternary Compounds," in *Springer Handbook of Electronic and Photonic Materials*, Springer International Publishing, 2017, pp. 1-1.

[14] T. C. Harman and A. J. Strauss, "Band Structure of HgSe and HgSe–HgTe Alloys," *Journal of Applied Physics,* vol. 32, p. 2265–2270, 1961.

[15] G. L. Klimchitskaya, U. Mohideen and V. M. Mostepanenko, "Kramers–Kronig relations for plasma-like permittivities and the Casimir force," *Journal of Physics A: Mathematical and Theoretical,* vol. 40, p. F339, 2007.